Interactions between metal cations and the ionophore lasalocid. Part 13.[1] Structure of 1:1 and 2:1 lasalocid anion–divalent cation complexes in methanol

Mostafa Mimouni,[a] Patrice Malfreyt,[a] Rachid Lyazghi,[a] Marc Palma,[a] Yves Pascal,[b] Gérard Dauphin[b] and Jean Juillard*,[a]

[a] *URA CNRS 434, Université Blaise Pascal, 63177 Aubière Cedex, France*
[b] *URA CNRS 485, Université Blaise Pascal, 63177 Aubière Cedex, France*

The successive formation of complexes MA^+ and MA_2 of alkaline-earth cations M^{2+} with lasalocid HA is observable in methanol. Knowing the corresponding formation constants, it was possible to access NMR parameters specific to these two types of species for the four alkaline-earth cations. ^{13}C and ^1H chemical shifts are reported for MA^+ and MA_2; ^1H–^1H coupling constants for MA^+ only. Experiments at low temperature and experiments using the paramagnetic cation Mn^{2+} determined the coordination sites. All these data show an appreciable variability of coordination in the series of alkaline-earth cations. Computations using the semi-empirical quantum methods AM1 and PM3 and Monte-Carlo simulations in methanol according to BOSS, mainly on MgA^+ and BaA^+ fully confirmed these findings.

The natural ionophore lasalocid (Fig. 1) is known to be able to transport both divalent and monovalent cations across

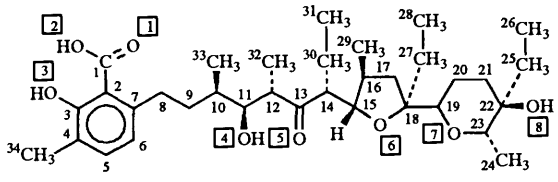

Fig. 1 Lasalocid formula with carbon and oxygen numbering scheme

membranes. With divalent cations, the formation at the water–membrane interface of a neutral complex able to migrate through the membrane is obviously a two step kinetic process involving successive formation of a 1:1 and then a 2:1 complex. In solvent systems, such as the water–chloroform biphasic system, only the complete reaction leading to the formation, from the ionophore HA and the cation M^{2+}, of the neutral salt MA_2, is observed in equilibrium studies. Both formation constants and structures of these species were recently investigated in the water–chloroform system for the whole alkaline-earth series.[1] Energies associated respectively with each of the two steps could not be derived from such work and how each of the two anions is implicated in the coordination of the cation cannot be stated with any certainty.

Studying equilibria in a more polar solvent affords the energies associated with the successive formations of the two species MA^+ and MA_2 and also provides some insight into their structure, *i.e.* the coordination sites of the cation and the conformation of the ligands. Standard or apparent thermodynamic functions for the reactions (1) and (2) were previously

$$A^- + M^+ \rightleftharpoons MA^+ \quad (1)$$

$$MA^+ + A^- \rightleftharpoons MA_2 \quad (2)$$

acquired in the solvent methanol for alkaline-earth cations ($\Delta G°$,[2] $\Delta H°$ and $\Delta S°$,[3] $\Delta C_P°$ and $\Delta V°$[4]) for some transition metal cations ($\Delta G°$,[5,6] $\Delta H°$ and $\Delta S°$[7]) and for some heavy metal cations ($\Delta G°$, $\Delta H°$ and $\Delta S°$[8]).

Knowledge of the equilibria then allows the predominant formation of either MA^+ or MA_2 in methanol to be favoured by acting on the respective concentrations of the components. NMR parameters corresponding to these two species could thus be obtained in CD_3OD. This was done for all the alkaline-earth cations. Previous work on ^{13}C and ^1H NMR of the free acid, anion and potassium salt of lasalocid in methanol[9] facilitated both acquisition and interpretation of these data. Using a paramagnetic cation, Mn^{2+}, yielded the coordination sites involved in these two species. All these experiments were expected to supply answers to the two questions: What are the structures of the two successive lasalocid complexes? How do they vary as a function of the cation? Additional data were obtained by modelling interactions and structures using quantum semi-empirical methods and Monte-Carlo simulations taking as a base our recent study on molecular modelling of lasalocid free acid and anion.[10]

Experimental

Chemicals

Lasalocid was obtained as previously;[2] likewise its tetraethylammonium salt.[4] Specification of alkaline-earth and manganese perchlorate samples used has already been stated.[4,5] The preparation of the neutral salts MA_2 was described in a recent paper.[1] Solvents CH_3OH and CD_3OD were as previously specified.[2,9]

NMR experiments

These were conducted as previously,[9] using the same apparatus (Bruker MSL 300) and methods.

Computations

Semi-empirical quantum calculations were carried out using AM1[11,12] and PM3[11–13] as stated in the last paper.[10]

Monte-Carlo statistical mechanics simulations were carried out with the BOSS[14] program. Atomic charges were first calculated using AM1 and then introduced in the parameter file. Except when otherwise stated, a first minimization was done in a continuum with a relative permittivity (dielectric constant), $D = 32.66$. The solute molecule was then placed with 378 methanol molecules[15] in a cubic cell (*ca.* 26.7 × 26.7 × 40 Å^3) with periodic boundary conditions. Metropolis[16] and preferential sampling[17] were used in the isothermal isobaric ensemble

at 25 °C and 1 atm. For these simulations equilibration was carried out for 3×10^6 configurations, volume being prevented from moving during the first 3×10^5 configurations, followed by averaging for 3×10^6 configurations. Intermolecular interaction energies were obtained using the AMBER/OPLS force field.[18] This force-field is constituted of intramolecular energy terms identical to those of the AMBER force-field [19] and inter- and intra-molecular energy terms between non-bonded atoms. These last interactions are represented by a Coulombic term and a Lennard-Jones 6, 12 term. For two molecules A and

$$\Delta E_{AB} = \sum_{i}^{\text{on A}} \sum_{j}^{\text{on B}} \left(\frac{q_i q_j e^2}{r_{ij}} + \frac{A_{ij}}{r_{ij}^{12}} - \frac{C_{ij}}{r_{ij}^{6}} \right)$$

B in which $A_{ij} = (A_{ii}A_{jj})^{\frac{1}{2}}$; $C_{ij} = (C_{ii}C_{jj})^{\frac{1}{2}}$; $A_{ii} = 4\,\varepsilon_{ii}\sigma_{ii}^{12}$; $C_{ii} = 4\,\varepsilon_{ii}\sigma_{ii}^{6}$, σ_{ii} and ε_{ii} being the usual Lennard-Jones parameters. The non-bonded contribution to the intramolecular energy is evaluated with the same expression for all pairs of atoms separated by more than three bonds.

Considering solute, solvent molecule and solvent box dimensions, the cut-off was set at 11 Å for both solute–solvent and solvent–solvent interactions. It was very large for intramolecular interactions in the solute. It was accepted that all C–C and C–O bonds could vary during the simulation. For each interaction the allowed change of each of the dihedral angles of lasalocid was set at less than 5° to limit the rejection rate of the generated structures; this rate was thus contained at about 40%.

All these computations were performed using a DECα3000/400S computer.

Results and discussion

^{13}C and ^{1}H NMR data on alkaline-earth lasalocid complexes

Two types of solutions were prepared. Type 1 resulted from dissolving the tetramethylammonium lasalocid salt and the metal perchlorate in CD_3OD analytical concentrations being respectively $c_A^* = 0.1$ mol dm^{-3} and $c_M^* = 0.2$ mol dm^{-3}. Assuming like formation constants in the two solvents CH_3OH and CD_3OD, calculations using constants previously obtained [2] show that in these conditions the MA^+ species is the predominant one (percentages from 96% for Mg^{2+} to 99.9% for Ba^{2+}). This was also obtained by dissolving the lasalocid metal salt MA_2 in CD_3OD and the metal chloride or perchlorate MX_2 in a 1:2 ratio (type 1′ solution). Type 2 solutions were obtained by dissolving the neutral lasalocid alkaline-earth salts at a concentration of 0.1 mol dm^{-3} in CD_3OD. Calculations using constant values previously reported [2] for the formation of both MA^+ and MA_2 gave the proportion in solution of the three species MA_2, MA^+ and A^-; percentages of A engaged in MA_2 lay between 76% for Ba^{2+} and 84% for Mg^{2+} in these concentration conditions.

All the ^{13}C and ^{1}H spectra obtained with these two types of solutions were well resolved, denoting rapid exchange between various species or between the two ligands involved in the same species. ^{13}C and ^{1}H resonance frequencies were independently and unequivocally assigned for each solution from the ^{1}H spectrum, the ^{13}C broad-band and J-mod spectra, the ^{1}H–^{1}H (COSY 45) and ^{13}C–^{1}H correlation contour plots as previously described.[9] ^{1}H and ^{13}C spectra corresponding to a 100% species were obtained by correcting for the presence of other species using $\delta = \Sigma_i r_i \delta_i$ in which δ is the actual experimental chemical shift, δ_i the chemical shift of species i and r_i the fraction of the total amount of the ionophore engaged in the species i. The MA^+ spectra were readily obtained from solutions of type 1 or 1′, which then gave the MA_2 spectra from solutions of type 2 with corrections for the presence of MA^+ and A^-.[9] These corrected values of ^{1}H and ^{13}C chemical shifts are reported in Tables 1 and 2.

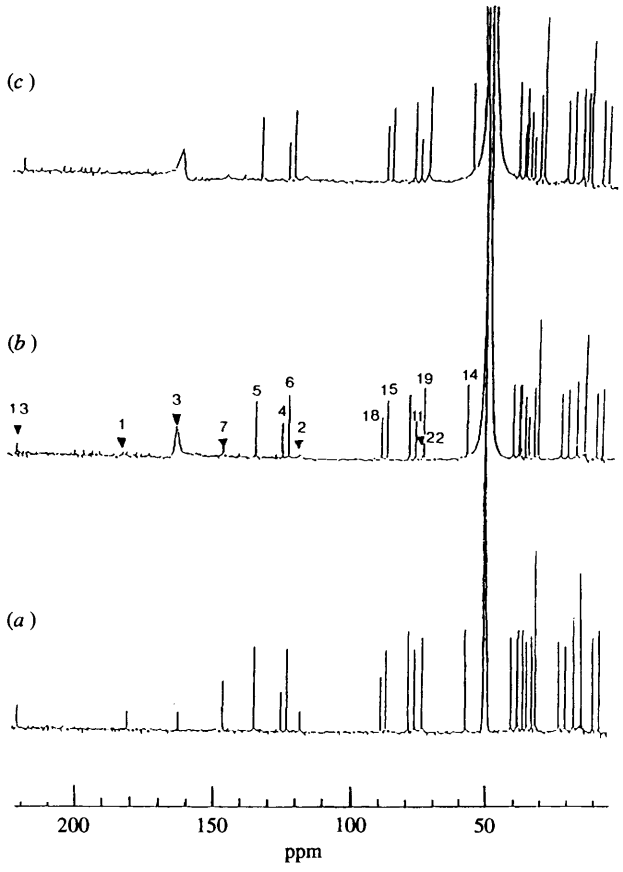

Fig. 2 ^{13}C spectra (^{1}H decoupled) in methanol of lasalocid–calcium 1:1 complex, CaA^+ alone (*a*) and in presence of manganese chloride (*b*, *c*) (ratio Mn/Ca = *r*). (*a*) $r = 0$ analytical concentrations $c^*(CaA_2) = 0.026$, $c^*(CaCl_2) = 0.14$ mol dm^{-3} which results in $c_{CaA^+} = 99.4\%$ and $c_{A^-} = 0.6\%$. (*b*) $r = 10^{-2}$. (*c*) $r = 4 \times 10^{-2}$.

^{1}H–^{1}H coupling constants were also obtained for the MA^+ species using procedures already reported.[9] Those which could be accessed are given in Table 3. No attempt was made to determine coupling constants for the MA_2 species since they would have been mean values for the two ligating anions.

Identification of the coordination sites was achieved using a paramagnetic cation Mn^{2+}. Both longitudinal and transverse relaxation times, T_1 and T_2, of a given carbon nucleus are affected by the presence in its neighbourhood of a paramagnetic cation. It is generally accepted that such interactions are mainly dipolar, enhancement of the relaxation times being related to the through-space carbon–cation distance. On the ^{13}C broad-band spectra, T_2 enhancement corresponds to signal broadening. The experiments conducted here were essentially qualitative; they were intended to provide information on the oxygens involved in the coordination. Starting from a solution in which the calcium species investigated, CaA^+ or CaA_2, is strongly preponderant, small amounts of $MnCl_2$ or MnA_2 were added. Formation constants of manganese or calcium lasalocid complexes are of the same order of magnitude;[2,5] sizes of the two cations Mn^{2+} and Ca^{2+} are similar. Thus gradual substitution of Ca^{2+} by Mn^{2+} could be expected. Effects observed in these experiments are presented in Figs. 2 and 3. No attempt was made to determine good values of T_2 or, better, of T_1 and by correlation to calculate metal-oxygen distances using Solomon and Bloembergen equations,[20] as done by Hanna *et*

Table 1 ^{1}H Chemical shifts for MA^+ and MA_2 complexes of lasalocid HA and alkaline-earth cations M^{2+} in methanol at room temperature

Proton	A^- [a]	MgA^+	MgA_2	CaA^+	CaA_2	SrA^+	SrA_2	BaA^+	BaA_2
5	7.03	7.27	7.08	7.09	7.07	7.08	7.05	7.08	7.05
6	6.57	6.79	6.66	6.61	6.61	6.61	6.60	6.62	6.58
8 A	3.36	3.40	3.29	3.31	3.35	4.00	3.62	4.17	3.76
8 B	2.94	3.09	3.02	2.99	2.95	2.32	2.71	2.24	2.56
9 A	1.73	1.76	1.76	1.76	1.72	1.83	1.78	1.77	1.79
9 B	1.55	1.62	1.68	1.61	1.56	1.65	1.60	1.69	1.66
10	1.75	1.76	1.72	1.76	1.72	1.83	1.78	1.87	1.79
11	3.99	4.03	4.01	4.02	4.04	4.64	4.28	4.62	4.35
12	3.04	2.96	3.04	3.13	3.08	3.16	3.08	3.13	3.09
14	2.83	2.87	2.84	2.99	2.95	3.16	2.97	3.09	2.94
15	3.87	3.82	3.87	3.92	3.90	3.83	3.86	3.97	3.96
16	2.14	2.28	2.20	2.26	2.25	2.46	2.30	2.49	2.32
17 A	1.88	2.03	1.89	1.96	1.92	2.07	1.98	2.08	1.98
17 B	1.71	1.52	1.72	1.67	1.72	1.65	1.62	1.69	1.66
19	3.60	3.66	3.61	3.75	3.69	3.87	3.73	3.88	3.76
20 A	1.73	1.76	1.72	1.76	1.72	1.83	1.78	1.84	1.83
20 B	1.53	1.62	1.54	1.61	1.56	1.65	1.60	1.77	1.66
21 A	1.64	1.87	1.68	1.76	1.72	1.83	1.67	1.84	1.79
21 B	1.50				1.56				
23	3.82	3.86	3.84	3.92	3.98	4.41	4.14	4.26	4.07
24	1.22	1.26	1.27	1.31	1.28	1.34	1.30	1.37	1.31
25 A	1.38	1.42	1.39	1.44	1.43	1.50	1.42	1.53	1.50
25 B									
26	0.97	0.96	0.98	0.94	0.93	1.07	0.98	1.09	1.03
27 A	1.67	1.87	1.72	1.76	1.78	2.07	1.96	2.08	1.83
27 B		1.42	1.54	1.52	1.56	1.50	1.58	1.58	1.56
28	0.91	0.93	0.94	0.99	0.97	0.96	0.94	0.97	0.94
29	1.06	1.14	1.08	1.11	1.09	1.16	1.10	1.17	1.12
30 A	1.97	1.95	1.97	1.96	2.00	2.07	2.02	2.08	1.98
30 B	1.57	1.44	1.54	1.61	1.56	1.65	1.60	1.69	1.56
31	0.93	0.93	0.94	0.98	0.97	0.96	0.93	0.94	0.87
32	0.99	1.04	1.00	1.03	1.02	1.14	1.06	1.13	1.08
33	0.94	1.03	0.97	0.99	0.98	0.99	1.03	0.99	0.97
34	2.19	2.26	2.23	2.20	2.22	2.22	2.22	2.22	2.21

[a] From ref. 9.

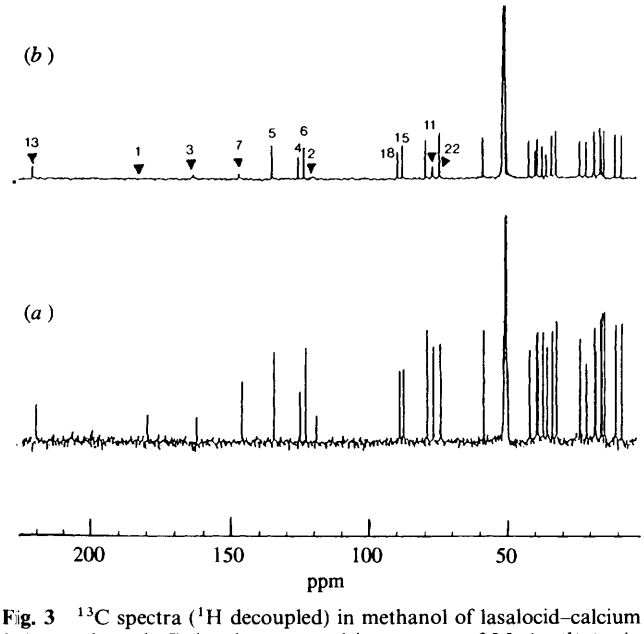

Fig. 3 ^{13}C spectra (^{1}H decoupled) in methanol of lasalocid–calcium 2 1 complex salt CaA_2 alone (*a*) and in presence of MnA_2 (*b*) (ratio Mn/Ca = *r*). (*a*) $r = 0$, analytical concentration $c^*(CaA_2) = 9.4 \times 10^{-2}$ mol dm^{-3} which results in $c_{CaA_2} = 76.2\%$, $c_A = c_{CaA^+} = 11.9\%$. (*b*) $r = 5 \times 10^{-3}$.

al.[21] and Lallemand *et al.*,[22] respectively for MnA_2 and CuA_2 in chloroform solution. This distance determination assumes[20] that interactions between the two nuclei M and C are mainly dipolar, which cannot be ascertained.

Structure of MA^+ complexes

It was thus possible from this data to obtain information on the structure of the two successive complexes of the divalent cations with the lasalocid anion in methanol. As suspected from thermodynamic data[3,7,8] actual structures are significantly dependent on the cation involved.

Structural aspects from NMR experiments. The relevant NMR data are clearly illustrated in Fig. 4 in which variations of ^{13}C chemical shifts in methanol from the free anion to its MA^+ complexes are considered. For a given carbon atom this variation is mainly related to interactions of the metal ion with a neighbouring oxygen atom, to conformational changes in its neighbourhood and, to a small extent, to local changes in the interactions with the solvent molecules. It is not very easy to attribute these chemical shift variations to particular causes. Nevertheless, it can be suggested from the strong positive variation of C-13 chemical shift that coordination of O-5 to Ba^{2+} and Sr^{2+} is very strong, to Ca^{2+} weaker and to Mg^{2+} very weak. From shift variations of C-15 and C-18, involvement of O-6 in the coordination of the cation is clear for Ba^{2+} and Sr^{2+}, still appreciable for Ca^+ and somewhat weak for Mg^{2+}. This conclusion could also be reached from Degani and Friedman's data;[23] analysis of the circular dichroism spectra of MA^+ at 290 mm, a wavelength for which the contribution of the ketone chromophore is large, showed a perturbation of the C=O group increasing with the size of the cation. From the effects observed on C-22, involvement of O-8 is suggested for

Table 2 ^{13}C Chemical shifts for MA^+ and MA_2 complexes of lasalocid HA and alkaline-earth cations M^{2+} in methanol at room temperature

Carbon	A^- [a]	MgA^+	MgA_2	CaA^+	CaA_2	SrA^+	SrA_2	BaA^+	BaA_2
1	175.9	177.2	177.2	180.0	178.7	177.1	177.6	177.1	177.0
2	119.3	117.6	117.8	116.8	117.7	117.6	118.2	117.6	118.5
3	161.1	160.7	160.8	161.4	161.3	161.7	161.3	161.7	161.4
4	123.4	124.8	123.8	123.8	123.8	124.0	123.7	124.0	123.8
5	132.6	135.5	133.4	133.6	133.3	133.3	133.0	133.3	132.9
6	121.3	122.5	121.7	121.6	121.6	121.7	121.4	121.7	121.4
7	144.8	144.7	145.1	145.1	145.1	144.6	144.7	144.6	144.7
8	34.1	34.9	34.0	33.8	34.0	33.1	33.7	33.1	33.7
9	38.1	38.1	37.8	37.7	37.9	37.7	37.9	38.1	38.3
10	35.6	35.6	35.4	35.4	35.4	34.3	35.0	34.4	35.0
11	75.5	75.8	75.4	76.3	75.4	72.5	74.2	72.1	74.0
12	49.6	50.3	49.7	50.4	50.2	50.1	50.0	49.9	50.0
13	217.8	218.6	217.7	221.3	219.3	225.5	221.6	225.1	222.0
14	57.6	55.8	57.2	56.5	56.9	56.1	56.8	56.3	57.2
15	85.5	85.1	85.7	86.0	86.2	86.2	85.9	87.3	86.3
16	37.8	35.7	37.5	36.9	37.1	35.2	36.5	35.5	36.5
17	41.0	38.9	40.7	39.7	40.2	38.5	39.6	38.1	39.5
18	86.8	88.1	88.0	88.2	87.8	89.3	88.3	90.2	88.8
19	73.5	71.2	73.2	72.4	72.7	71.4	72.2	71.6	72.5
20	22.1	20.6	22.0	21.9	21.9	21.2	21.5	20.9	21.4
21	30.2	30.5	30.3	30.3	30.4	30.0	30.2	30.5	30.4
22	72.1	72.3	72.1	73.0	72.7	73.7	72.9	73.8	73.3
23	77.8	77.4	77.7	78.0	77.6	76.7	77.4	77.7	77.9
24	14.8	14.3	14.8	14.4	14.5	13.6	14.2	13.6	14.2
25	32.2	32.7	32.2	31.9	32.1	31.9	32.0	31.9	32.1
26	6.8	6.7	6.8	6.7	6.8	6.6	6.8	6.6	6.9
27	30.8	31.0	30.7	31.1	30.5	30.5	30.5	30.5	30.6
28	8.8	9.6	8.8	9.0	9.1	9.8	9.3	9.8	9.3
29	16.9	15.8	16.2	16.3	16.6	15.5	16.3	15.5	16.1
30	19.7	17.2	19.5	19.4	19.6	17.3	18.6	17.0	18.2
31	12.7	12.2	12.8	13.0	13.0	12.0	13.2	12.1	12.8
32	14.2	13.4	14.2	13.7	13.9	13.6	13.2	13.6	13.1
33	13.0	12.8	12.9	13.0	13.1	12.4	12.7	12.4	13.4
34	16.2	15.8	16.6	16.0	16.2	16.2	16.1	16.2	16.2

[a] From ref. 9.

Table 3 Vicinal proton coupling constants for MA^+ complexes of lasalocid HA with cations M^{2+}

	Experimental (in methanol)					Computational				
						Gaseous state		Methanol [b]		
	MgA^+	CaA^+	SrA^+	BaA^+	A^- [a]	I_2(AM1)	I_{Mg}(PM3)	I_{Mg}(BOSS)	X_{Mg}(BOSS)	I_{Ba}(BOSS)
8A–9A	2.4	4.4	3	2.3	4.0	2.3	4.4	2.0	2.2	2.3
8A–9B	12.6	11.2	12.0	11.3	11.2	12.3	12.7	11.7	12.8	12.4
8B–9A	10.2	11.7	11.0	12.0	11.2	12.3	12.7	11.7	10.7	12.3
8B–9B	6.0	5.2	4.5	5.0	5.6	5.6	4.4	6.7	6.4	5.3
10–33	7.0	6.0	6.0	6.8	6.5	7.2	7.2	7.2	7.2	7.2
10–11	1.2	1.5	1.5	2.2	1.8	3.1	2.0	3.2	1.7	3.7
11–12	10.2	9.7	10.5	10.2	10.0	9.9	10.1	9.9	10.3	10.2
12–32	7.2	7.2	7.2	7.5	7.0	7.0	7.0	7.0	7.0	7.0
14–30A	10.8	10.4	11.3	11.3	10.0	11.9	12.1	11.9	10.8	12.2
14–30B	2.4	3.9	—	3	4.0	2.3	2.5	2.3	2.4	4.6
14–15	1.2	3.3	3	1.5	4.0	1.8	2.6	1.6	1.6	3.4
15–16	10.8	7.4	10.5	10.5	10.0	7.4	7.9	5.7	10.7	10.3
16–17A	7.0	5.2	7.0	6.0	8.0	7.0	9.0	6.0	6.9	6.7
16–17B	4	8.3	9.2	10.5	11.0	10.4	9.3	10.8	9.4	11.5
16–29	6.3	6.4	6.0	6.5	6.5	7.2	7.2	7.2	7.2	7.2
19–20	5.4	7.5	9.0	11.3	10.0	11.2	11.2	10.8	5.4	10.9
19–20B	2.4	3.0	3.5	3	3.2	3.7	3.2	4.8	2.3	4.8
23–24	7.2	7.0	7.2	7.5	7.0	6.4	6.4	6.4	6.4	6.5
25–26	7.0	7.6	7.2	7.5	7.0	7.5	7.5	7.5	7.5	7.5
27–28	7.5	7.2	7.6	7.0	6.8	7.5	7.5	7.5	7.5	7.5
30–31	7.5	6.5	7.6	7.8	6.8	7.5	7.5	7.5	7.5	7.5

[a] From ref. 9. [b] Mean values using a Boltzman distribution.

Ba^{2+}, Sr^{2+} and, to a lesser extent for Ca^{2+}, not clearly for Mg^{2+}. For O-1 or O-2, appreciable variations observed on C-4, C-5 and C-6, probably related to transmission of electronic effects across the benzene ring suggest a stronger coordination of Mg^{2+} than other cations. Nevertheless, the strong effects observed on C-1 and C-2 for Ca^{2+} are also noteworthy.

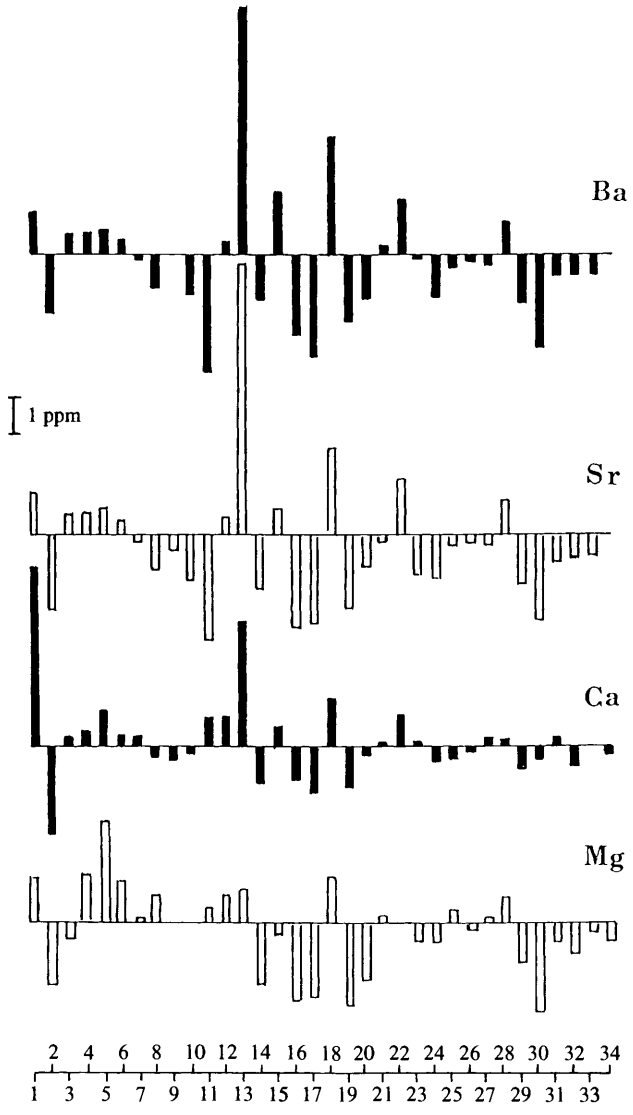

Fig. 4 Variation in the ^{13}C chemical shifts of all the carbon atom of lasalocid from its free anion A^- to its 1:1 complexes MA^+ in methanol. $\delta\ ^{13}C\text{-}n$ (A in MA^+) $-\ \delta\ ^{13}C\text{-}n$ (A in A^-) from C-1 to C-34.

Appreciable conformational changes appear on the area C-9, C-12 for BaA^+ and SrA^+, not for CaA^+ or MgA^+ and on the C-13, C-15 area for MgA^+, BaA^+ and SrA^+ but weakly for CaA^+ (as shown by C-14 and C-30 chemical shift variations). Concerning the two heterocycles, conformational changes are suggested for the four cations though they must be weaker for CaA^+, maximal variations being observed for the furan ring (on C-16, C-17) in BaA^+ and for the pyran ring (on C-19 and C-20) in MgA^+. This last observation is supported by data on ^1H–^1H coupling constants. On the whole, from the ^{13}C chemical shift, the smallest conformational changes from A^- to MA^+ would seem to be observed for CaA^+. ^1H–^1H coupling constants' values are in close agreement with this for the aliphatic part of the molecule from C-8 to C-15 but not for the rings for which a marked deformation of both the furan and the pyran rings are observed in CaA^+. Examination of 19-H, 20-H coupling constants suggest an inversion of the pyran ring for MgA^+, the structure observed in A^- only being found in BaA^+. These two constants show intermediate values for CaA^+ and SrA^+ which suggest either twist forms or resonance between the two chair forms.

NMR experiments involving Mn^{2+} yield information on the coordination sites of the cation in MnA^+ the structure of which is expected to be not very different from that of CaA^+ in methanol. Adding $MnCl_2$ to a solution of type 1 in CD_3OD containing mainly CaA^+ (concentration ratio $c^*_M/c^*_A \simeq 0.04$) resulted, as shown in Fig. 2, in the disappearance of C-1, C-2, C-7 and C-22 signals and broadening of C-3 and C-13 signals, which suggests a closed form of the molecule through main coordination of Mn^{2+} in MnA^+ by O-1 or O-2, O-5 and O-8.

Computational studies. Modelling the structure of MA^+ complexes was first attempted in a vacuum using quantum semi-empirical methods. Firstly, a doubly charged 'sparkle' of radius 0.7 Å was introduced in some of the geometries previously derived [10] for the lasalocid anion, its initial location being somewhat subjective. Structure optimization was carried out using either AM1 or PM3,[11] two versions of a quantum semi-empirical method derived from MNDO.[12,13] According to the starting situation and the program used various geometries were obtained. Their formation energies, of the order of 645 kcal mol^{-1}, lie, taking into account a systematic difference related to parametrization differences between PM3 and AM1, in a 2 kcal mol^{-1} margin. However their structures differ appreciably. Nevertheless, some general features concerning the coordination of the cation modelled by this sparkle are observed: O-1 and O-2 are both coordinating sites, standing at a distance of the order of 3 Å from the cation. Coordination to O-5 is significant, distances from the sparkle to this oxygen being with high regularity of the order of 3.5 Å. The terminal oxygen O-8 is frequently at a distance of 4 Å from the cation, though in some cases the O(8)H···O(1) hydrogen bond is retained. Distances to the sparkle from O-4, O-6 and O-7 range from 4.1 to 4.8 Å, those of the oxygens nearest to the cation being variable. As an example, results for a structure I_2 obtained using anion geometry I_a [10] and AM1 program optimization are reported in Tables 3 and 4. Such a structure corresponds closely to coordination features previously described for MnA^+; the cation is mainly bound to O-1 and O-2, O-5 and O-8. Corresponding ^1H–^1H coupling constants were calculated using the Durette and Horton formula [24] as previously.

Substituting the Mg^{2+} cation (which is parametrized in PM3) for the 2^+ sparkle affords very spectacular results. Starting from closed geometry I_2 here described in Tables 3 and 4, after optimization using PM3, gave I_{Mg}—also described in these Tables and presented in Fig. 5. A very strong coordination of Mg^{2+} by the carboxylate, which results in a marked shortening of the M···O-1 and M···O-2 distances (up to 1.85 Å) is observed. This corresponds to a strong opening of the structure, the nearest potentially coordinating oxygens being O-5 and then O-4 and O-8 but at distances greater than 4.5 Å. Calculation of the ^1H–^1H coupling constants, as shown in Table 3, gave values consistent with the experimental ones for MgA^+ except for the rings. Other computed MgA^+ conformations also present the same general trends: strong coordination of the magnesium cation to the carboxylate and breaking of head–tail hydrogen bonds of the ligand.

The above computations are for the gaseous state. To compare experimental data Monte-Carlo simulations were carried out in methanol using the program BOSS as described in the experimental part. Given interpretations proposed for thermodynamic data [3] and the present results, it was considered important to make the size of the cation variable. All alkaline-earth cations were parametrized, according to Aqwist [25] in the program used but, to save computer time, investigations were restricted here to the smallest and largest of these cations, the structural features observed thus being assumed to be representative of two extreme situations.

The initial geometry of BaA^+ was derived from X-ray data for a $BaA_2{\cdot}2H_2O$ crystal.[26] The second anion ligand and the

Table 4 Parameters for various structures of MA^+ species obtained using 2^+ sparkle, Mg^{2+} or Ca^{2+} cation and resulting, in the gaseous state from quantum semi-empirical calculations (AM1 or PM3) and in methanol from Monte-Carlo simulations (BOSS): metal cation–lasalocid oxygen and C(1)–C(22) distances, hydrogen bond length (all distances in Å), conformation of the rings, steric angle θ between benzene and carboxylate planes, mean number of methanol molecules in the first and second solvation shells of cation n_1 and n_2 with corresponding oxygen–cation mean distances d_1 and d_2.

	I_2(AM1)	I_{Mg}(PM3)	I_{Mg}(BOSS)	X_{Mg}(BOSS)	I_{Ba}(BOSS)
M···O-1	3.3	1.8	3.3 ± 0.2	1.9 ± 0.1	5.7 ± 0.6
M···O-2	2.8	1.8	1.8 ± 0.1	1.9 ± 0.1	3.9 ± 0.5
M···O-4	4.8	5.1	4.2 ± 0.2	4.8 ± 0.1	4.1 ± 0.5
M···O-5	3.5	4.6	4.5 ± 0.3	6.3 ± 0.2	3.3 ± 0.9
M···O-6	4.3	6.0	5.7 ± 0.3	7.7 ± 0.3	3.8 ± 0.7
M···O-7	4.3	5.8	4.5 ± 0.2	7.3 ± 0.3	3.5 ± 0.3
M···O-8	3.5	5.3	3.0 ± 0.2	4.4 ± 0.2	3.4 ± 0.7
O8-H···O1	2.3	6.1	3.1	5.2	2.4
O8-H···O2	4.2	6.4	3.5	3.9	2.5
O3-H···O1	2.0	1.8	2.1	2.0	2.4
C(1)···C(22)	5.4	7.7	5.9	6.5	4.8
THF	*a*	Twist	Twist	Twist	Twist
THP	Chair	Chair	Chair	Chair	Chair
θ (deg)	−39	−4	−39	−24	−19
n_1, n_2			3.0, 3.0	4.0, 3.1	5.0, 4.2
d_1, d_2 (Å)			1.93, 4.2	2.08, 4.0	2.75, 4.8

[a] Between twist and envelope.

water molecules were withdrawn and the protons were located optimally; meanwhile care was taken to maintain the O(8)···H···O(1) hydrogen bond. A chloride ion was also added to the cell, but at a sizeable distance to ensure system electroneutrality and also to avoid interactions between this ion and the ionophore–barium complex. Computations for the BaA^+ complex gave a globular geometry I_{Ba} depicted in Fig. 6, in which the cation is coordinated to oxygens of the ligand. Corresponding relevant parameters are given in Tables 3 and 4. In this structure, the anion ligand is closed through hydrogen bonding O-8 to both O-1 and O-2 roughly equivalently. It thus wraps the cation, all the oxygens of the crown being involved to some extent in its coordination (Fig. 5) in agreement with experimental features for the ^{13}C chemical shifts. Calculated ^1H–^1H coupling constants agree acceptably with experimental ones.

For the magnesium complex, various computations were also carried out using the BOSS program. A Mg^{2+} cation was substituted for the sparkle in the previous form I_2 (AM1). After optimization in a continuum the resulting geometry was then placed in the methanol molecule box. Equilibration resulted in geometry I_{Mg}(BOSS) depicted in Fig. 7. Significant Mg···O mean distances are also reported in Table 4. Comparison of the ^1H–^1H mean coupling constants to the accessible experimental ones revealed some structural inadequacies for both this geometry and geometry I_{Mg}(PM3). Discrepancies mainly concern the THF ring [C(15)–C(16) bond] and the THP ring [C(19)–C(20) bond]. Observed coupling constants J_{19-20} clearly result from an inversion, compared to other lasalocid species, of the THP ring; this inversion for example does not occur, as shown in Table 3, for the BaA^+ complex. Accordingly, starting from the I_2(AM1) geometry, an inversion of the THP cycle was carried out and dihedral angles were thus fitted to values calculated from known ^1H–^1H coupling constants. This was done using an appropriate procedure in the SYBYL package.[29] The resulting geometry was thus directly placed in methanol. Equilibration resulted in geometry X_{Mg}(BOSS) the parameters of which are also presented in Tables 3 and 4. As expected, an improved agreement was found between experimental and calculated ^1H–^1H coupling constants for MgA^+ in methanol. Mg^{2+} strongly bound to the carboxylate group. In comparison coordination to the other oxygens of the ligand is rather weak. A small opening of the structure is observed. These features previously shown by calculations using PM3 are thus confirmed by Monte-Carlo simulations in methanol.

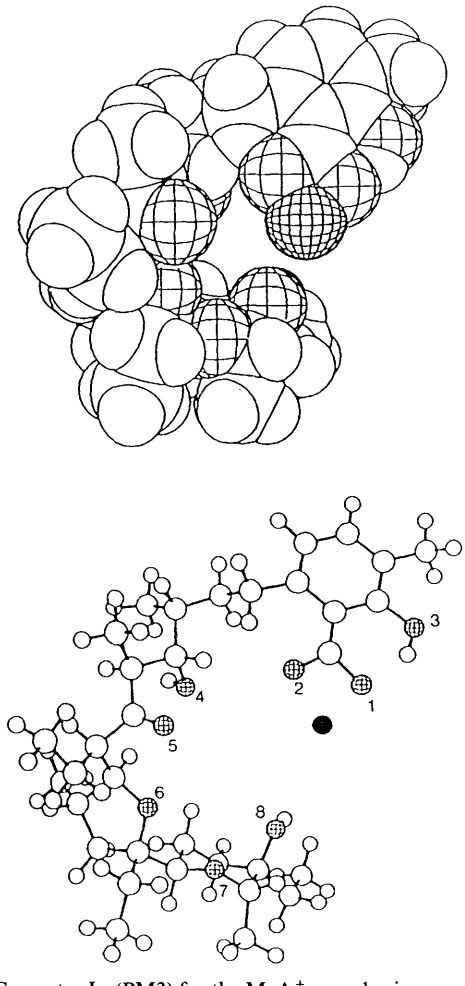

Fig. 5 Geometry I_{Mg}(PM3) for the MgA^+ complex in a vacuum using semi-empirical quantum calculation with program PM3 as described. ○ carbon, ○ hydrogen ⊕ oxygen ● metal cation.

Concerning the method, it must be stressed that conformation I_{Ba} and I_{Mg} were first optimized, using the AMBER/OPLS

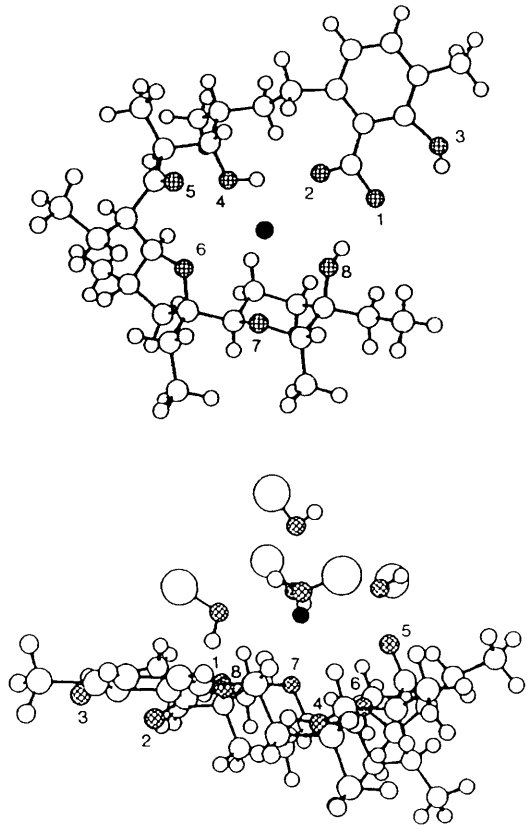

Fig. 6 Geometry I_{Ba}(BOSS) for the BaA^+ complex in methanol using Monte-Carlo simulation in methanol. Top: a view showing the coordination of Ba^{2+} by the oxygens of the ligand. Bottom: a view showing the coordination of Ba^{2+} to both the lasalocid anion and the five nearest methanol molecules.

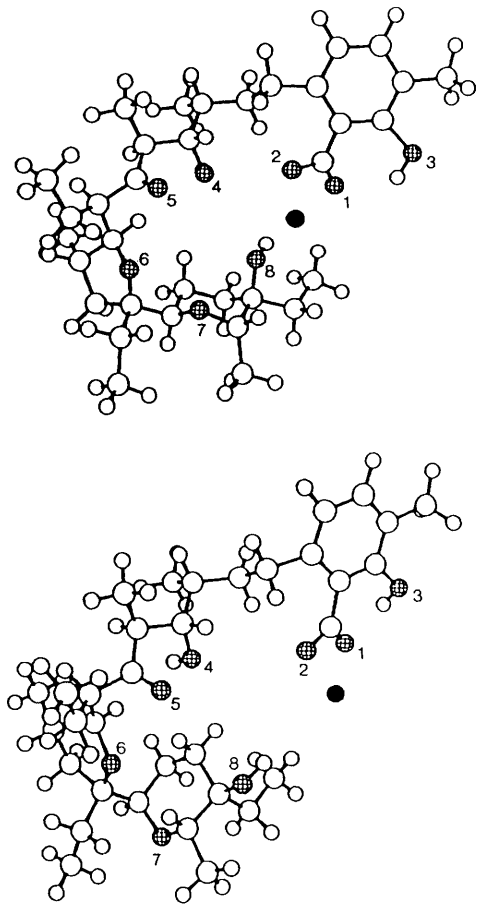

Fig. 7 Skeleton schemes of geometry I_{Mg} (top) and X_{Mg} (bottom) of MgA^+ in methanol resulting both from Monte-Carlo simulations using BOSS

force-field in a dielectric continuum ($\varepsilon = 32.66$). These conformations are thus expected to correspond at least to local enthalpy minima. Monte-Carlo computations using the 'preferential sampling option' mainly act on the first solvation shell solvent molecule distribution and on the cation location, little on the solute, the initial optimized geometry of which is barely modified. On 3×10^6 configurations, enthalpies and their standard deviations for systems ($MA^+ + Cl^- + 378$ MeOH) were found to be respectively -3738 ± 4 kcal mol^{-1} for conformation I_{Ba}, -3881 ± 4 for conformation I_{Mg} and -3845 ± 3 for conformation X_{Mg}. The low values of the standard deviations show that the configurations retained during the sampling are narrowly scattered, which suggests that these systems can be considered as equilibrated. Calculations of the enthalpies of association of MA^+ in methanol from these data and analogous data for separate M^{2+} and A^- ions yield to unrealistic values, compared with the experimental ones;[3] not surprising considering Jorgensen's own statement[27] that searching for enthalpy differences of less than 10 kcal mol^{-1} is currently impractical. Differences observed between enthalpies of systems I_{Mg} and X_{Mg} have also to be noted. The X_{Mg} conformation is more compatible with structural data but its enthalpy appears in this computation as less favourable. Would its entropy be more favourable?

Monte-Carlo simulations using BOSS also showed that the desolvation of the alkali-metal cations is only partial in the MA^+ complexes. Fig. 8 shows the radial distribution function between the cation involved and the methanol molecule oxygen atoms. They are compared to analogous radial distribution functions, obtained in comparable conditions, for the cation alone. By integration of the first two peaks of these radial distribution functions, mean numbers of near neighbouring methanol molecules n_1 in the first and n_2 in the second solvation shells of the cation were calculated. They are also reported in Table 4 along with corresponding cation–methanol oxygen mean distances, respectively d_1 and d_2. Corresponding computed values for free cations in methanol are $n_1 = 8.3, d_1 = 2.8$, $n_2 = 8.2, d_2 = 5.0$ for Ba^{2+} and $n_1 = 6.0, d_1 = 2.0, n_2 = 6.1$, $d_2 = 4.1$ for Mg^{2+}. Concerning this last cation it is interesting to observe the close agreement between these values and those resulting from X-ray diffraction studies and molecular dynamic simulation of a 0.6 mol dm^{-3} solution of $MgCl_2$ in methanol by Tamura *et al.*[28] The height of the peak corresponding to the second solvation shell differs appreciably in the two simulations; this could be due to differences in solvent model, expression of interaction energies and concentrations; however, integration of the two peaks results in analogous values of methanol molecule number in this second shell: between 6 and 7.

Concerning MgA^+ and BaA^+ complexes it can be observed in Fig. 8 that the radial distribution function tends to 1 as expected when r increases, consistent with good equilibration of the system.

Concluding on the MA^+ structure in methanol. On the basis of the comparison of standard thermodynamic functions associated with MA^+ complex formation for lasalocid and salicylic acid in methanol, it was previously suggested that[3] going from magnesium to barium, the cation shifted from a location opposite the carboxylate group to one in the centre of the pseudo-crown. Also, examination of the electronic absorption spectrum of the salicylate chromophore revealed that[3] the salicylate moiety in lasalocid MA^+ complexes became less involved as the size of the cation increased. Both are

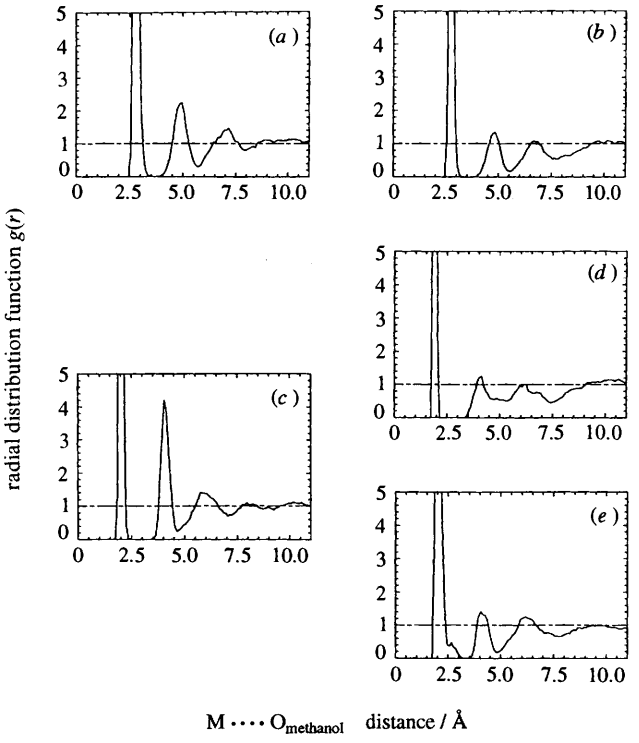

Fig. 8 Radial distribution functions $g(r)$ as a function of the metal cation–methanol oxygen (M^{2+}–O) distance r in Å. (*a*) Ba^{2+} alone in methanol. (*b*) Ba^{2+} in the BaA^+ complex in methanol (geometry I_{Ba} BOSS). (*c*) Mg^{2+} alone in methanol. (*d*) Mg^{2+} in the MgA^+ complex in methanol (geometry I_{Mg} BOSS). (*e*) As (*d*) (geometry X_{Mg} BOSS).

supported here. From both NMR data and computational modelling, Ba^{2+} is coordinated to O-5, O-6, O-7 and O-8 and weakly to O-2. Conversely, Mg^{2+} is strongly bound to the carboxylate and weakly to O-8 and O-4. Coordinating systems of other cations are intermediate as clearly shown by the ^{13}C chemical shift patterns in Fig. 4. The structure of SrA^+ is very near that of BaA^+. Coordination to the carboxylate clearly occurs with Ca^{2+} concurrently with a weakening of the cation coordination to O-5, O-6 and O-8. Experiments with the paramagnetic cation Mn^{2+} show main coordination to the carboxylate, O-5 and O-8. Thus the wide variability of the coordination of the cation by lasalocid anion is confirmed. This variation is clearly a function of the size of the cation which determines continuous changes in both conformation of the ligand and involvement of the coordination sites.

One of the aspects of this concerns the conformation of the pyran cycle. Continuous variations with the size of the cation from BaA^+ to MgA^+ result in a complete inversion of the cycle from BaA^+ to MgA^+. Owing to its better fit to the experimental ^1H–^1H coupling constants, geometry X_{Mg} should correspond at best to the actual structure of MgA^+ in methanol. However, the modelling does not reveal why, whether because of steric hindrance or interactions, such an inversion of the pyran ring is favoured.

Results in Table 4 and Fig. 6 stress the importance of the residual solvation of the cation in the MA^+ complexes. Some of the molecules of the solvent, by completing the coordination shell of the cation, contribute to the stability of these complexes. In the case of MgA^+ the strong remaining solvation of the cation, probably also contributes to appreciable opening of the structure.

Structure of 2:1 complexes MA_2. Owing to budgetary constraints on both programs and computers, computational simulations involving two ligating molecules such as in MA_2 complexes could not be carried out. Structural information concerning these species are thus derived only from NMR experiments. At ambient temperature ^{13}C and ^1H spectra of MA_2 complex salts are well resolved for all species studied, which denotes either a symmetric role of the two A^- ligands or their rapid exchange. Complementary experiments were carried out at low temperature (240 to 220 K) on calcium type 2 solutions, in which mainly CaA_2 was present. With respect to reference signals, such as those of the methyl carbons, an appreciable broadening of signals corresponding to C-11, C-13 and C-10, C-17 and C-18 and also C-20 was observed. This can be taken as a sign of the dissymetric role played by the two A^- ligands in CaA_2, their exchange being slower at low temperature. Moreover, these results suggest analogous coordination of the cation by the carboxylate and O-8 and possibly the O-6 and O-7 of the two ligands and specific involvement of O-4 of one ligand and O-5 of the other one.

Analogous conclusions can be drawn from experiments with Mn^{2+}. Adding small amounts of either $MnCl_2$ or MnA_2 to a solution of type 2 containing mainly CaA_2 had identical effects: C-1, C-2, C-3, C-7; C-8, C-9, C-10; C-11; C-13; C-22 signals disappeared or were markedly broadened, which again suggests the involvement of O-1 or O-2, O-4, O-5 and O-8 borne by one or the other of the two anions ligands. O-4, which is not involved in coordination in the MnA^+ complex, thus appears to be in MnA_2. C-15, C-18 and C-19, C-23 signals are not appreciably affected, which suggests that O-6 and O-7 are not strongly involved in the coordination of Mn^{2+} in MnA_2.

The two anion ligands thus have different conformations. At ambient temperature what are observed in spectra are mean parameters for the two anion ligands involved in the complexation of the cation. Structural information on these two ligating anions can nevertheless be obtained assuming that adding the second molecule does not perturb the first one. In these conditions, assuming for example that ^{13}C chemical shifts of the first molecule $(A^-)'$ are those of A^- in MA^+, the ^{13}C chemical shifts can be calculated for the second molecule $(A^-)''$. If this is done, it appears that except in the case of Mg^{2+}, $(A^-)''$ exhibits only very small differences from free anion A^- in methanol. Some perturbations nevertheless occurring in C-1, C-2, C-31 and C-32 suggest that the main involvement is that of the oxygens of the carboxylate. However, examination of data resulting from experiments involving Mn^{2+} and experiments concerning CaA_2 at low temperature suggest for these two cations an involvement of the O-4 of the second molecule in their coordination. In addition, it must be mentioned that contrary to what was observed in chloroform [1] for SrA_2 and BaA_2 no significant shift of H-28, expected to result from the cycle current of the benzene ring of the other molecule, occurs here. The structure of the MA_2 species in methanol must then be a more open one than in chloroform. The second molecule $(A'')^-$ acts as a rather mobile lip of a bowl formed by the first molecule $(A')^-$ and hosting the cation.

References

1 Part 12, R. Lyazghi, Y. Pointud, G. Dauphin and J. Juillard, *J. Chem. Soc., Perkin Trans. 2*, 1993, 1681.
2 J. Juillard, C. Tissier and G. Jeminet, *J. Chem. Soc., Faraday Trans. 1*, 1988, **84**, 951.
3 Y. Pointud, E. Passelaigue and J. Juillard, *J. Chem. Soc., Faraday Trans. 1*, 1988, **84**, 1713.
4 J. Woznicka, C. Lhermet, N. Morel-Desrosiers, J.-P. Morel and J. Juillard, *J. Chem. Soc., Faraday Trans. 1*, 1989, **85**, 1709.
5 P. Laubry, C. Tissier, G. Mousset and J. Juillard, *J. Chem. Soc., Faraday Trans. 1*, 1988, **84**, 969.
6 P. Laubry, G. Mousset, P. Martinet, M. Tissier, C. Tissier and J. Juillard, *J. Chem. Soc., Faraday Trans. 1*, 1988, **84**, 3175.
7 Y. Pointud and J. Juillard, *J. Chem. Soc., Faraday Trans. 1*, 1990, **86**, 3395.

8 M. Mimouni, Y. Pointud and J. Juillard, *Bull. Soc. Chim. Fr.*, 1994, **131**, 58.
9 R. Lyazghi, A. Cuer, G. Dauphin and J. Juillard, *J. Chem. Soc., Perkin Trans. 2*, 1992, 35.
10 P. Malfreyt, Y. Pascal and J. Juillard, *J. Chem. Soc., Perkin Trans. 2*, 1994, 2031.
11 Program MOPAC *v.* 6.0, QCPE n° 455 (Dept. Chem., Indiana University), according to refs. 12 and 13.
12 M. J. S. Dewar, E. G. Zoebisch, E. F. Healy and J. J. P. Stewart, *J. Am. Chem. Soc.*, 1985, **107**, 3902.
13 J. J. P. Stewart, *J. Comput. Chem.*, 1989, **10**, 209.
14 W. L. Jorgensen, BOSS *v.* 3.4, Yale University, New Haven, CT, 1991.
15 W. L. Jorgensen, *J. Phys. Chem.*, 1986, **90**, 1276.
16 N. Metropolis, A. W. Rosenbluth, M. N. Rosenbluth, A. Teller and E. J. Teller, *J. Chem. Phys.*, 1953, **21**, 1087.
17 W. L. Jorgensen, *J. Phys. Chem.*, 1983, **87**, 5304.
18 W. L. Jorgensen and J. Tirado-Rives, *J. Am. Chem. Soc.*, 1988, **110**, 1657.
19 S. J. Weiner, P. A. Kollman, D. A. Case, V. C. Singh, C. Ghio, G. Alagena, S. Profeta and P. Wernier, *J. Am. Chem. Soc.*, 1984, **106**, 765.
20 I. Solomon and W. Bloembergen, *J. Chem. Phys.*, 1956, **25**, 261.
21 D. A. Hanna, C. Yeh, J. Shaw and C. W. Everett Jr., *Biochemistry*, 1983, **22**, 5616.
22 J. Y. Lallemand, R. Rao and T. Prangé, *Nouv. J. Chim.*, 1980, **4**, 315.
23 H. Degani and H. L. Friedman, *Biochemistry*, 1974, **13**, 5022.
24 P. L. Durette and D. Horton, *Org. Magn. Reson.*, 1971, **3**, 417.
25 J. Aqwist, *J. Phys. Chem.*, 1990, **94**, 8021.
26 I. H. Suh, K. Aoli and H. Yamazaki, *Acta Crystallogr., Sect. C*, 1989, **45**, 415.
27 W. J. Jorgensen, B. Bigot and J. Chandrasekha, *J. Am. Chem. Soc.*, 1982, **104**, 4584.
28 Y. Tamura, E. Spohr and K. Heinziger, *Ber. Bunsenges. Phys. Chem.*, 1992, **96**, 147.
29 Tripos Associates, 1699 S. Hanley Road, suite 303, St. Louis, MO, 63144, Sybyl 6.03, 1993.

Paper 4/07870E
Received 29*th December* 1994
Accepted 7*th June* 1995